ROCSCIENCE

CPillar

Factor of Safety Calculations – Voussoir Analysis (Rectangular Pillar)

Theory Manual

Table of Contents

1. Introduction 3

2. Crown Pillar Geometry 4

2.1. Rectangular Pillar 4

3. Voussoir Equations 5

3.1. Effective Unit Weight 5

3.2. Arch Height 5

3.3. Maximum Confining Stress 6

3.4. Midspan Displacement 6

4. Shear Strength 7

4.1. Normal Stress 7

4.2. Shear Strength 7

4.2.1. Mohr Coulomb 7

4.2.2. Hoek-Brown 8

4.2.3. Generalized Hoek-Brown 9

5. Factor of Safety 10

5.1. Voussoir Analysis 10

5.1.1. Shear Factor of Safety 11

5.1.2. Arch Snap-Thru Probability 12

5.1.3. Compression Factor of Safety 13

6. References 14

1. Introduction

This paper documents the calculations used in *CPillar* to determine the shear failure and elastic buckling factors of safety for surface or underground crown pillars, and laminated roof beds. This involves the following series of steps:

1. Determine the crown pillar geometry
2. Determine the horizontal and vertical stress state of the soil/rock
3. Determine the normal stresses on the abutments
4. Solve for Voussoir critical values by iteration
5. Compute the resisting forces due to abutment shear strength
6. Calculate the safety factor(s) and probabilities of failure

2. Crown Pillar Geometry

2.1. Rectangular Pillar

A rectangular pillar is defined by its length (x), width (y), and thickness (z). A thickness of overburden (t_o) can also be added above the pillar. The height of water (h_w) can be specified to any height above the base of the pillar.

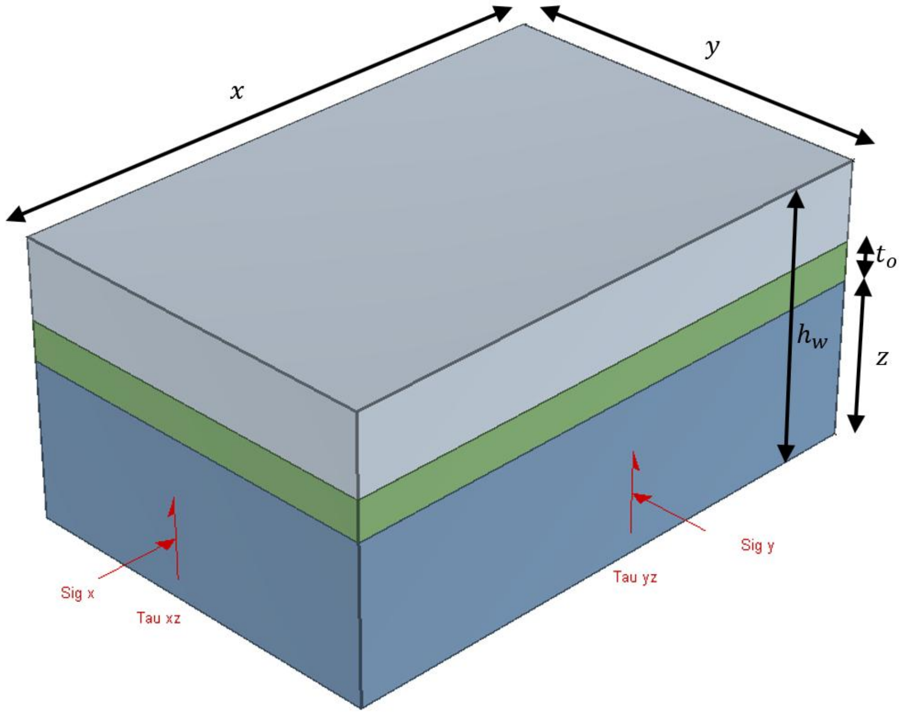

Figure 2.1-1: Rectangular Pillar Geometry

Where:

x is the pillar length

y is the pillar width

z is the pillar height

t_o is the thickness of overburden above the pillar

h_w is the height of water from the base of the pillar

γ_r is the rock unit weight

γ_o is the overburden unit weight

γ_w is the water unit weight

3. Voussoir Equations

CPillar uses an iterative process to calculate the Voussoir values.

3.1. Effective Unit Weight

The driving forces responsible for the destabilization of the crown pillar is attributed by the weight of the entire system.

The effective unit weight of the pillar is computed as follows:

$$\gamma_{eff} = \gamma_r \cos\theta_{fd} + \gamma_o \frac{t_o}{z}\theta_{fd} - \frac{P}{z} \tag{1}$$

Where:

γ_{eff} is the effective unit weight of the pillar

γ_r is the unit weight of rock (pillar)

θ_{fd} is the face dip angle

γ_o is the unit weight of overburden

t_o is the thickness of overburden

z is the height of the pillar

P is the support pressure

Note: Water pressure and loads are not considered in a VOUSSOIR analysis.

3.2. Arch Height

$$h_{arch} = \sqrt{\frac{3az_{check}}{8}} \tag{2}$$

with

$$z_0 = z\left(1 - \frac{2n}{3}\right) \tag{3}$$

$$L = a + \frac{8{z_0}^2}{3a} \tag{4}$$

$$f_{av} = \frac{1}{3}\sigma_{c_{max}}\left(\frac{2}{3} + n\right) \tag{5}$$

(Diederichs and Kaiser, 1999)

$$dL = \frac{f_{av}(1 - kv)L}{E_{rm}} \tag{6}$$

$$z_{check} = \frac{8{z_0}^2}{3a} - dL \geq 0 \tag{7}$$

3.3. Maximum Confining Stress

$$\sigma_{c_{max}} = \frac{\gamma_{eff}a^2\left(0.25 - k\frac{a}{3b}\right)}{nh_{arch}} \quad \text{with} \quad k = \frac{a}{2}\left[\sqrt{\left(\frac{a}{b}\right)^2 + 3} - \frac{a}{b}\right] \tag{8}$$

3.4. Midspan Displacement

$$\Delta_{mid} = z_0 - h_{arch} \tag{9}$$

Where:

h_{arch} is the arch height

a is the breadth of the pillar (longer dimension)

v is Poisson's ratio

E_{rm} is the rock mass modulus

n is the relative thickness (with respect to pillar thickness) of the compression arch

$\sigma_{c_{max}}$ is the maximum induced lateral compressive stress

Δ_{mid} is the midspan displacement

4. Shear Strength

The resisting forces are provided by the shear strength along the abutments of the pillar.

4.1. Normal Stress

The normal stresses to the abutments:

$$N = \frac{\sigma_{c_{max}}}{2} \tag{10}$$

Where:

N are the normal stresses along the abutments

$\sigma_{c_{max}}$ is the maximum induced lateral compressive stress

4.2. Shear Strength

The following shear strength criteria are available in *CPillar* for defining the strength of the rock:

1. Mohr-Coulomb
2. Hoek-Brown
3. Generalized Hoek-Brown

4.2.1. Mohr Coulomb

$$\tau = c + N \cdot \tan \phi \tag{11}$$

Where:

c is the cohesion

N is the normal stress along the abutments

ϕ is the friction angle

4.2.2. Hoek-Brown

Note that this is a special case of the **Generalized Hoek-Brown** criterion, with the constant a = 0.5.

$$\sigma_1' = \sigma_3' + \sigma_{ci}\left(m_b\frac{\sigma_3'}{\sigma_{ci}} + s\right)^{0.5} \tag{12}$$

(Hoek and Bray, 1981)

If $s = 0$:

$$\tau = 0$$

If $s \neq 0$:

$$\tau = \left(\frac{1}{\tan\phi_i} - \cos\phi_i\right)\frac{m_b\sigma_{ci}}{8}$$

with

$$\phi_i = \tan^{-1}\left(\frac{1}{\sqrt{4h\cos^2\theta - 1}}\right)$$

$$h = 1 + \frac{16(m_b * N + s * \sigma_{ci})}{3{m_b}^2\sigma_{ci}}$$

$$\theta = \frac{1}{3}\left(\frac{\pi}{2} + \tan^{-1}\frac{1}{\sqrt{h^3 - 1}}\right)$$

Where:

m_b is a reduced value (for the rock mass) of the material constant *mi* (for the intact rock)

s is a constant which depends upon the characteristics of the rock mass

σ_{ci} is the uniaxial compressive strength (UCS) of the intact rock pieces

σ_1' is the axial effective principal stress

σ_3' is the confining effective principal stress

4.2.3. Generalized Hoek-Brown

Generalized Hoek-Brown (m_b, s, a):

$$\sigma_1' = \sigma_3' + \sigma_{ci}\left(m_b \frac{\sigma_3'}{\sigma_{ci}} + s\right)^a \tag{13}$$

(Hoek and Bray, 1981)

Check for tensile strength:

$$\sigma_t = -\frac{s\sigma_{ci}}{m_b}$$

If $N < \sigma_t$:

Generalized Hoek-Brown (GSI, mi, D):

$$m_b = m_i \exp\left(\frac{GSI - 100}{28 - 14D}\right) \tag{14}$$

$$s = \exp\left(\frac{GSI - 100}{9 - 3D}\right) \tag{15}$$

$$a = \frac{1}{2} + \frac{1}{6}\left[\exp\left(-\frac{GSI}{15}\right) - \exp\left(-\frac{20}{3}\right)\right] \tag{16}$$

Where:

m_b	is a reduced value (for the rock mass) of the material constant *mi* (for the intact rock)
s, a	are constants which depend upon the characteristics of the rock mass
σ_{ci}	is the uniaxial compressive strength (UCS) of the intact rock pieces
σ_1'	is the axial effective principal stress
σ_3'	is the confining effective principal stress
GSI	is the Geological Strength Index
m_i	is a material constant for the intact rock
D	is a "disturbance factor" which depends upon the degree of disturbance to which the rock mass has been subjected by blast damage and stress relaxation (varies from 0 for undisturbed in situ rock masses to 1 for very disturbed rock masses)

5. Factor of Safety

5.1. Voussoir Analysis

For a VOUSSOIR analysis, three failure modes are considered:

1. Shear (vertical slippage at abutments),
2. Arch Snap-thru (buckling due to gravity), and
3. Localized Crushing Failure.

For a VOUSSOIR (no tension) analysis, a rectangular roof is assumed to be divided by cracking into trapezoidal and triangular panels, corresponding to lines of maximum principal tensile stress of an elastic stress analysis. This is illustrated in plan-view in Figure 5.1-1. Such cracking is analogous to the yield lines postulated in the behaviour of reinforced concrete slabs.

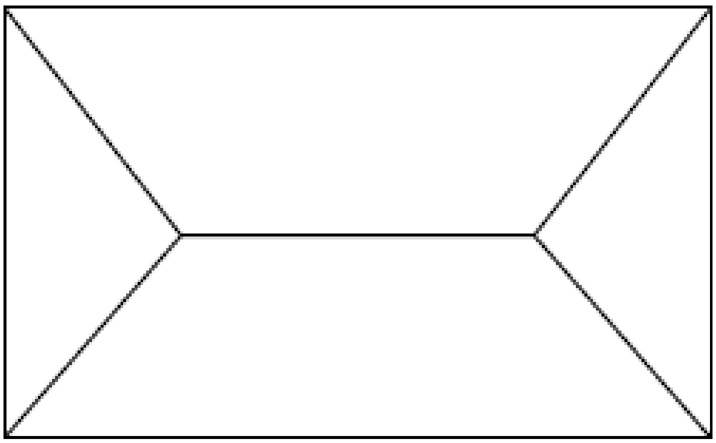

Figure 5.1-1: Yield Lines for a Rectangular Roof Plate (Plan View)

For a long excavation ($x \gg y$ or $y \gg x$) this configuration approximates plane strain conditions with a longitudinal crack at midspan. For a square excavation, four equal triangular panels result.

5.1.1. Shear Factor of Safety

The shear factor of safety from a VOUSSIOR analysis balances the shear strength of the long excavation dimension against the weight of a trapezoidal panel. This scheme automatically incorporates long or square excavations in the limiting cases of $x = y$ or $x \gg y$ or $y \gg x$. Unlike the RIGID and ELASTIC analyses, the shear strength of the short excavation dimension (and the weight of the smaller "triangular" panels) does not enter into the shear stability calculation.

Since the lateral compressive stress is solely induced by the arching action of the rock and is not due to external field stresses, low span-to-depth ratios will result in low shear factor of safety values, since the rock cannot develop the lateral stress required for a self-supporting arch. This is why span-to-depth ratios less than 3 are not recommended for a VOUSSOIR analysis.

The maximum shear strength is computed based on the maximum arch compressive strength from the Voussoir iteration procedure.

$$FS_{shear} = \frac{shear\ resistance}{dead\ load} = \frac{2\tau_{max} n b}{\gamma_{eff}\, a(b-k)} \tag{17}$$

with

$$k = \frac{L_{span}}{2}\left[\sqrt{\left(\frac{a}{b}\right)^2 + 3} - \frac{a}{b}\right]$$

Where:

FS_{shear}	is the shear factor of safety
τ_{max}	is the maximum shear strength
a	is the breadth of the pillar (longer dimension)
b	is the span of the pillar (shorter dimension)
n	is the relative thickness (with respect to pillar thickness) of the compression arch
γ_{eff}	is the effective unit weight of the pillar

5.1.2. Arch Snap-Thru Probability

This is the primary failure mode of interest in a VOUSSOIR analysis. The essential feature of a roof supported by a Voussoir action are illustrated in Figure 2.1-1, for a horizontal beam. Deflection has been exaggerated for purposes of illustration.

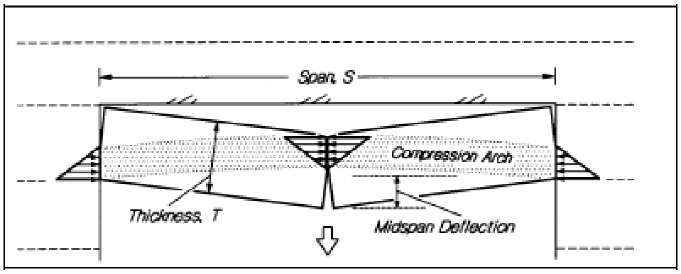

Figure 5.1-2: Problem Geometry for Voussoir Stability Analysis (Hutchinson et al., 1996)

Like elastic buckling, "arch snap-thru" is highly dependent on geometry (span/depth ratio) and rockmass modulus. However, the driving force for gravity buckling is the self-weight of the rock, whereas the driving force for elastic buckling is the externally applied lateral stress. As such, they are entirely different modes of failure, although both are referred to as buckling failure modes.

The **buckling parameter** calculated in a Voussoir analysis represents the percentage of unstable arch configurations for a given geometry and rock mass modulus, as determined by the Voussoir analysis iteration procedure. A buckling parameter = 35% has been determined Hutchinson et al. (1996) as a limit above which a roof should be considered unstable. This design limit of 35% happens to correspond to midspan deflection = 10% of the beam thickness. Therefore, arch stability can also be assessed by monitoring the displacement at midspan, relative to the undeflected state. The average displacement at midspan (for all statistical combinations of input parameters) is displayed along with the arch snap-thru statistics.

Failure probabilities (Voussoir analysis) corresponding to mean buckling parameter ranges

Table 5.1-1: Failure Probabilities (Voussoir Analysis) Corresponding to Mean Buckling Parameter Ranges

Failure Probability	Mean Buckling Parameter
LOW	0-10
MEDIUM	10-25
HIGH	25-50
VERY HIGH	> 50

Note: The design curves of Beer & Meek (1982) correspond to the *CPillar* solution when the buckling parameter (in *CPillar*) just reaches 100 (i.e. 99 to 100). This represents a mathematically critical state which will lead to collapse at the slightest disturbance, and as such is not a conservative design limit. The *CPillar* recommended limit for arch snap-thru stability (buckling parameter < 35) is based on a more conservative but realistic approach to the Voussoir concept of roof stability. See Hutchinson et al. (1996) for full details.

5.1.3. Compression Factor of Safety

The iterative procedure used in a Voussoir analysis is considered to have converged when a stable minimum value of the induced lateral compressive stress can be determined. This is the stress which holds the arch in place. It arises from considering the moment equilibrium of the driving and resisting force couples acting on the arch.

Triangular stress distributions are assumed to act at the arch abutments and at the arch midspan, keeping the arch in place. The most stable configuration for the Voussoir arch is that which **minimizes** the **maximum** stresses of these assumed triangular distributions.

If this stress **exceeds the uniaxial compressive strength of the rock**, localized crushing failure is considered to have occurred, and arch snap-thru may follow, even though the primary snap-thru analysis may indicate a stable arch.

$$FS_{crushing} = \frac{\sigma_{ci}}{\sigma_{c_{max}}} \tag{18}$$

Where:

σ_{ci} is the uniaxial compressive strength (UCS) of the intact rock pieces

$\sigma_{c_{max}}$ is the maximum induced lateral compressive stress

The crushing (or compression) factor of safety will usually be quite high. It will only become a failure mode issue in its own right under certain conditions, when the uniaxial compressive strength is very low. Depending on the scale of the rock volume involved, and the presence of planes of weakness inclined at some angle from the lateral stress direction, the effective uniaxial compressive strength for the roof may be significantly lower than the value for the intact rock specimens. Thus, the potential for compressive failure should be based on the minimum value of uniaxial compressive strength to be expected for the transversely isotropic lithological unit (Beer et al., 1982).

For rocks with low compressive strength, the critical displacement at midspan may be less than 10% of the beam thickness (Hutchinson et al., 1996).

6. References

1. Beer, G. and Meek, J.L. Design curves for roofs and hanging-walls in bedded rock based on "voussoir" beam and plate solutions. Trans. Instn. Min. Metall. 91, 1982, pp A18-A22.
2. Brady, B.H.G. and Brown, E.T. Rock Mechanics for Underground Mining (2nd Edition) (Chapter 8), London: Allen and Unwin, 1993, 571 pages.
3. Duncan, J.M. (2000). Factors of safety and reliability in geotechnical engineering. J. Geotechnical & Geoenvironmental Engineering, April, pp. 307-316.
4. Evans, W.H. The strength of undermined strata. Trans. Instn. Min. Metall., 50, 1941, 475-532.
5. Hoek, E. (1989) A Limit Equilibrium Analysis of Surface Crown Pillar Stability. Proc. Int. Conf. on Surface Crown Pillars Active & Abandoned Metal Mines Timmins, pp. 3-13.
6. Hoek, E. Lessons from Case Histories in Rock Engineering. Course notes, Dept. of Civil Engineering, University of Toronto, Toronto, Ontario, Canada, 1992, pp 71-79.
7. Hoek, E. and Brown, E.T. The Hoek-Brown Failure Criterion - a 1988 Update. 15th Canadian Rock Mechanics Symposium, 1988, pp 31-38.
8. Hutchinson, D.J. and Diederichs, M. (1996). Cablebolting in Underground Mines, Vancouver: Bitech. 400 pages.
9. Law, A.M. and Kelton, D.W. (1991). Simulation Modeling and Analysis (2nd edition), McGraw-Hill, Inc., New York.
10. Rosenbleuth, E. Point estimates for probability moments. Proc. Nat. Acad. Sci. 10, 1972, pp 3812-3814.
11. Timoshenko, S. and Woinowsky-Kreiger, S. (1987). Theory of Plates and Shells (2nd ed.). McGraw-Hill Book Company, Inc.